



OPEN T cell induced expression of Coronin-1A facilitates blood-brain barrier transmigration of breast cancer cells

Johan M. Kros^{1✉}, Lona Zeneyedpour², Rute M. S. M. Pedrosa¹, Zineb Belcaid¹, Willem A. Dik³, Theo M. Luiders² & Dana A. M. Mustafa¹

In previous work we discovered that T lymphocytes play a prominent role in the rise of brain metastases of ER-negative breast cancers. In the present study we explored how T lymphocytes promote breast cancer cell penetration through the blood brain barrier (BBB). An in vitro BBB model was employed to study the effects of T lymphocytes on BBB trespassing capacity of three different breast carcinoma cell lines. Differential protein expression was explored by comparing the proteomes of the breast cancer cells before and after co-culture with activated T lymphocytes using liquid chromatography-mass spectrometry (LC-MS). siRNA was used to silence protein expression in the breast cancer cells to study contribution to in vitro BBB passage. Furthermore, protein expression in primary breast cancer tissues was explored and related to brain-metastatic potential. Co-culturing with activated T lymphocytes or their conditioned medium (CM) resulted in increased passage through the in vitro BBB. The effects were less for cell line MDA-MB-231-B2M2 (brain affinity) as compared to MDA-MB-231 and SK-BR-7. Mass spectrometry-based proteomics revealed significant alterations in the expression of 35 proteins by the breast cancer cell lines upon T cell contact. Among the proteins is coronin-1A, a protein related to cell motility. Knockdown of *CORO1A* in the breast cancer cells reduced their ability to cross the artificial BBB to 60%. The effects were significantly less for the cell line derived from breast cancer with affinity for brain. The expression of coronin-1A was confirmed by immunohistochemistry and RT-PCR of 52 breast cancer samples of patients with metastasized breast cancers, with and without brain locations. Lastly, *CORO1A* upregulation was validated in a publicly available mRNA expression database from 204 primary breast cancers with known metastatic sites. We conclude that T lymphocytes trigger cancer cells to express proteins including coronin-1A that enable the cancer cells to cross an in vitro BBB. In addition, a prominent role of coronin-1A in the formation of cerebral metastases in breast cancer patients is strongly suggestive by its upregulation in tissue samples of breast cancer patients with brain metastases.

Keywords Breast cancer, Brain metastasis, Blood–brain barrier, Proteomics, Liquid chromatography-mass spectrometry, Coronin-1A

Abbreviations

BBB	Blood–brain barrier
CM	Conditioned medium
CORO1A	Gene coding for the protein coronin-1 A
coronin-1A	Protein encoded by CORO1A
DNA	Deoxyribonucleic acid
DMEM	Dulbecco modified eagle medium
ECM	Endothelial cell medium
ER	Estrogen receptor

¹Department of Pathology, The Tumor Immuno-Pathology Laboratory, Erasmus University Medical Center, Wytemaweg 80, 3000 DR Rotterdam, The Netherlands. ²Department of Neurology, Laboratory of Neuro-Oncology, Clinical and Cancer Proteomics, Erasmus University Medical Center, Wytemaweg 80, 3000 DR Rotterdam, The Netherlands. ³Laboratory Medical Immunology, Department of Immunology, Erasmus University Medical Center, Wytemaweg 80, 3000 DR Rotterdam, The Netherlands. ✉email: j.m.kros@erasmusmc.nl

FFPE	Formalin-fixed paraffin-embedded
GEO	Gene expression omnibus
HSA	Human serum albumin
HCMDB	Human cancer metastasis database
HUVEC	Human umbilical vein endothelial cell
LC-MS	Liquid chromatography-mass spectrometry
mRNA	Messenger RNA
NCBI	National Center for Biotechnology Information
RNA	Ribonucleic acid
ROI	Region of interest
RPMI	Roswell Park Memorial Institute cell medium
RT-PCR	Reverse transcription polymerase chain reaction
siRNA	Small interfering RNA
TCGA	The Cancer Genome Atlas

More than 30% of patients suffering from common cancers will develop brain metastatic disease and incidences are rising^{1,2}. Treatment options for these patients are limited and unfortunately, preventive strategies to this most serious complication of cancer are lacking. In order to invade the brain, cancer cells need to pass the blood–brain barrier (BBB). The mechanisms that tumor cells utilize to take this hurdle are largely undiscovered. Since distinct variation in brain metastatic potential between different tumors exist^{1–4}, lineage-specific differences in crossing the BBB have been suggested. In a previous study we discovered prominent involvement of the T cell response in the formation of the brain metastases in ER-negative breast cancer⁵. We used an artificial BBB to model the facilitating effect on passage of cultured tumor cells following contact with activated T cells. Moreover, also in *in vivo* studies by employing an immunocompetent mouse model, the incubation of tumor cells with T cells significantly enhanced the passage of the tumor cells through the BBB, resulting in predominant formation of brain metastases⁵.

In the present study we investigated if the effects of activated T lymphocytes on the passage of tumor cells through the *in vitro* BBB also occurs for breast cancer cell lines with different brain affinities. Specifically, we examined two breast cell lines that are known to develop brain metastasis and one cell line that is described to not induce metastases. By comparisons of the cancer cell proteomes before and after T cell contact we sought commonly upregulated proteins. Additionally, the effect of coronin-1A, a protein prominently identified with a well-known function in cellular migration, was tested in the *in vitro* BBB model by RNA knockdown on the transmigration through the BBB.

Methods

Breast cancer cell lines

The MDA-MB-231 cell line is ER, PR, and E-cadherin negative and expresses mutated p53 and was isolated from an invasive ductal carcinoma⁶. The MDA-MB-231 genome clusters with basal subtype of breast cancer. The cells lack HER2 and are commonly used as a model for triple-negative breast cancer. MDA-MB-231 cells are known to seed to lymph nodes upon orthotopic transplantation in mice. Various cell lines derived from MDA-MB-231 were selected for specific metastatic predilection among which line MDA-MB-231-B2M2 that preferentially metastasizes to brain⁷. The SK-BR-3 (SKBR3) cells were isolated in 1970 from pleural effusion of a breast adenocarcinoma patient. This cell line overexpresses Her2 and is a preferential model for Her2 positive breast cancer with metastatic potential without organ-specificity⁸.

Cell line culture procedure

Human astrocytes (ScienCell) were cultured in astrocyte medium (AM, ScienCell) supplemented with 1% astrocyte growth factors (AGS, ScienCell), 2% fetal bovine serum (FBS, ScienCell), and 1% penicillin and streptomycin (P/S, ScienCell). Human umbilical vein endothelial cells (HUVECs, ScienCell) were cultured in endothelial cell medium (ECM, ScienCell) supplemented with 1% endothelial cell growth factors (ECGS, ScienCell), 5% FBS, and 1% P/S. Human astrocytes and HUVECs were used between passage 2 and 5. Breast cancer cell lines were cultured in RPMI-1640 with L-glutamine (BioWhittaker) medium supplemented with 10% FBS and 1% P/S, and 1% gentamicin was added to the breast cancer cells. All cell lines were cultured at 37 °C, in a humidified incubator with 5% CO₂.

Activation and expansion of T-lymphocytes

Human bulk T lymphocytes isolated from healthy donors were expanded on irradiated allogeneic feeder cells, consisting of a mixture of 40-Gy gamma-irradiated peripheral blood mononuclear cells, Epstein-Barr Virus (EBV)-transformed B-lymphoblast cell lines BSM (also known as GM06821, GLCneg/HLA-A2pos) and APD (also known as GM06817, EADneg/HLA-A1pos) cells. Cells were cultured in RPMI-Hepes (Gibco) with 1% L-glutamine (BioWhittaker), 1% P/S and 6% human serum albumin (HSA), in combination with phytohemagglutinin-L (PHA-L, Sigma) and IL-2 in a 96-well flat-bottomed plate for 6–7 days at 37 °C, in a humidified incubator with 5% CO₂. After incubation, cells were harvested, centrifuged, and cultured in RPMI-Hepes medium supplemented with 6% HSA and IL-2 (360 IU/mL, Chiron, Amsterdam, The Netherlands).

Construction of the *in vitro* blood-brain barrier (BBB) model

The specifications of the BBB *in vitro* model were published. The BBB model was assembled as described before^{5,9}. In short, HUVECs were co-cultured with human astrocytes on opposite sides of a transwell insert. Twenty-four-wells transwell polycarbonate inserts (surface area 0.33 cm², pore size 3 μm, Becton Drive, Franklin

Lakes, NJ, USA) were coated with 2% gelatin (Sigma) for 45 min. The transwell inserts were placed upside-down and ~100,000 human astrocytes/inserts were seeded at the bottom side of the inserts. The cells were allowed to adhere for 3 h at 37 °C in a 5% CO₂ incubator and were fed every 15–30 min. After 3 h, inserts were flipped and placed in 24-well plates. One mL of astrocyte media was added to the lower chamber and astrocytes were allowed to grow for one day. Fifty-thousand endothelial cells were plated on the upper chamber of the inserts and the cultures were placed in the incubator for three days. The permeability of the BBB model was verified by adding trypan blue dye to the upper chamber and incubating the model for 30 min at 37 °C. Medium from the lower chamber was collected and absorbance was measured at 595 nm. The permeability of the BBB model by trypan blue was included in duplicate in each experiment.

HUVECs were co-cultured with human astrocytes on the opposite sides of a transwell insert⁹. Inserts with pore sizes of 3.0 µm were used. In order to prevent direct cell-cell contact for part of the experiments, a 0.4 µm pore membrane physical barrier between both cell types was applied, or following incubation of the tumor cells with the T lymphocyte CM.

Functional studies using the in vitro BBB

To investigate the influence of T lymphocytes on the ability of the various cancer cells to cross the BBB, three parallel sets of experiments were conducted: (1) cancer cells were co-cultured with T lymphocytes in a 3:1 ratio to investigate the effects of direct cell-cell contacts; (2) cancer cells were cultured with cell-free conditioned media (CM) from activated T lymphocytes to investigate the effects of activated T lymphocyte-derived soluble factors; (3) cancer cells cultured without the addition of T lymphocytes, or T lymphocyte CM, were used as controls. Co-culturing was performed for five consecutive days at 37 °C, with 5% CO₂. The culturing procedure and visualization of passed cells are described previously⁵.

Cell pellet preparation for LC-MS and RT-PCR measurements

Co-culturing experiments were repeated twice for proteomics and genomics measurements. Following the first five days of the co-culture procedure, the T lymphocytes were removed by three consecutive vigorous PBS-washing steps. The tumor cells were trypsinized, collected into sterile tubes, and washed with PBS in six consecutive steps. During the last wash step, cells were collected in 1.5 ml Eppendorf tubes, centrifuged for 5 min at 1000g, and the presence of residual T cells was excluded by screening for CD3, CD4, and CD8. The supernatant was removed and the cell pellets were snap-frozen in dry ice and stored at – 80 °C until further use.

Protein digestion and proteomics measurements

Frozen cell pellets were re-suspended in 50 µL 0.1% RapiGest buffer (Waters Corporation, Milford, MA) and cells were disrupted by external sonification for one minute at 70% amplitude at a maximum temperature of 25 °C (Branson Ultrasonics, Danbury, CT). A reducing agent, 0.5 M DL-dithiothreitol (Sigma-Aldrich), was added to a final concentration of 5 mM and the samples were incubated at 60 °C for 30 min. Iodoacetamide (Sigma-Aldrich) alkylating reagent was added to a final concentration of 15 mM and samples were kept in the dark for 30 min. For protein digestion to each sample, 0.5 µg trypsin gold, mass spectrometry grade (Promega, Madison, WI), was added and incubated overnight at 37 °C. To stop the digestion, the pH of the solution was adjusted to pH < 2 with trifluoroacetic acid (TFA, Sigma-Aldrich) to a final percentage of 0.5%. Protein samples were incubated at 37 °C for 30 to 45 min. Subsequently, these samples were spun at maximum speed for 40 min at 4 °C. The supernatant was transferred into sterile LC-vials to be measured with LC-MS, as previously described⁵.

Proteomics data analysis

Samples were measured with LC-MS and raw data files from the Orbitrap Fusion mass spectrometer were processed as described before⁵. Scaffold software (The Industry Standard DDA MS/MS Proteomics Tool version 5.3.2, Portland, OR, <https://www.proteomesoftware.com/products/scaffold-5>) was used to identify peptides and proteins as previously described⁵. Identified proteins of each type of breast cancer cell lines that were co-cultured with either activated T lymphocytes or T-lymphocyte CM were compared to those of cancer cells cultured without the addition of activated T lymphocytes or T-lymphocyte CM. The comparison was based on t-test between two groups using Excel and Anova analysis among three groups using Scaffold software, and the p values of all proteins were considered differentially expressed if $p < 0.05$. The mass spectrometry proteomics data have been deposited to the ProteomeXchange Consortium via the PRIDE¹⁰ partner repository with the dataset identifier PXD053787 and <https://doi.org/10.6019/PXD053787>. The selection procedure of relevant proteins was based on significant expressional difference before and after T lymphocyte or CM contact and functional properties related to cell migration and/or cell locomotion. In order to verify the absence of T lymphocytes in the samples, specific proteins relating to T lymphocyte lineage were screened with proteomics (Table S2).

siRNA knockdown

A mix of four siRNA sequences that target *CORO1A* mRNA (5'-CCUCAAGGAUGGCUACGUA-3', 5'-CCAU GACAGUGCCUCGAAA-3', 5'-CCGCAAAGGCACUGUCGUA-3' and 5'-GUGCAGUGUUCGUGUCGGA-3') and scrambled non-targeting siRNAs (5'-UGGUUUACAUGUCGACUAA-3', 5'-UGGUUUACAUGUUGU GUGA-3', 5'-UGGUUUACAUGUUUCUGA-3' and 5'-UGGUUUACAUGUUUCCUA-3') were obtained from Dharmacon (GE health care, Netherland). Breast cancer cells were transfected following the manufacturer's protocol (using Lipofectamine[®] RNAiMAX Reagent, Invitrogen). The efficiency of *CORO1A* knock-down was assessed after 24 and 72 h, at mRNA and protein levels. Random siRNAs were used as siSHAM negative controls for silencing.

Immunofluorescence microscopy

Breast cancer cells were trypsinized and 5×10^4 cells were fixed in formaldehyde for 15 min and kept in 100% ethanol until cytocentrifugation and staining with an antibody against coronin-1 A (1:250, sc-100925, Santa Cruz Biotechnology). Cells from two independent experiments were analyzed by confocal microscopy using a LSM700 Zeiss microscope (Zeiss, Oberkochen, Germany). Images were captured with a 20× lens and a 4 × 4 tile was made from each slide. Each image was divided in 16 individual microscopic fields from which signal intensity as a mean \pm SD was determined using ImageJ software¹¹.

Breast cancer tissue sample selection

Primary ER- breast cancer FFPE samples from patients who developed brain metastasis ($n=23$) and from patients who developed metastases to other organs, excluding brain metastases ($n=29$) were collected. None of the breast cancer patients received neoadjuvant therapy (clinical information of $n=20$ samples has been previously provided in⁵, and from the validation set $n=32$ in¹²). This study was approved by the Medical Ethics Committee of the Erasmus Medical Center, Rotterdam, The Netherlands (MEC 02-953) and performed in adherence to the Code of Conduct of the Federation of Medical Scientific Societies in the Netherlands (<http://www.fmwv.nl/>).

Morphological assessment of breast cancer samples

Hematoxylin and eosin (H&E)-stained 5- μ m-thick sections from each sample, prepared before and after sectioning for RNA isolation and IHC, were evaluated by an experienced pathologist. Tumor cell areas were selected microscopically and a minimum content of 60% tumor tissue was taken as a threshold for RNA isolation.

Reverse transcription-polymerase chain reaction (RT-PCR)

Total RNA was extracted from frozen cell pellets using the RNeasy Plus Micro kit (Qiagen, Hilden, Germany) and from FFPE patient material, extracted from 10 to 15 five μ m sections (depending on the size of the sample) using the RNeasy FFPE Micro kit (Qiagen, Hilden, Germany), according to manufacturer's protocols. The quantity and quality of the isolated RNA were assessed (2100 Bioanalyser, Agilent Technologies, Santa Clara, USA). Samples were excluded if the yield did not reach a minimum of 100 ng RNA/ μ l. Reverse transcription was performed using the RevertAid H-Minus first-strand cDNA synthesis kit (Thermo Scientific, Vilnius, Lithuania) according to the manufacturer's protocol. Quantitative real-time PCR (RT-PCR) was performed using TaqMan Master Mix (Applied Biosystems, Austin, USA) on the 7500 RT-PCR system, v.2.3 (Applied Biosystems, Foster City, USA). The following commercially available exon-spanning TaqMan Gene Expression Assays (Applied Biosystems, California, USA) were used: *CORO1A* (Hs00200039_m1), *HPRT1*, exon 2–3 (Hs02800695_m1) and *HMBS*, exon 13–14 (Hs00609296_g1). *HPRT1* and *HMBS* were used as reference genes. The relative quantification of target gene expression was performed using the $2^{-\Delta\Delta Ct}$ comparative method.

Immunohistochemistry

Anti-coronin-1A (1:2000, sc-100925, Santa Cruz Biotechnology) antibody was used according to the manufacturer's instructions. All IHC slides were scanned on a Nano-zoomer 2.0HT scanner (40× magnification, Hamamatsu Photonics, Japan) and four tumor regions of interest (ROI's) per slide were randomly selected. ROI's were evaluated with a semi-quantitative IHC method²³. In short, ImageJ Fiji 1.52p software (USA) was used to deconvolute the selected immunostained ROI's and convert the slides into gray shades. Finally, intensity scores are based on the mean grey value per ROI's and total area intensity ratio of each specific IHC coronin-1A staining. All four ROI's per slide were implemented in the evaluation.

Publicly available mRNA expression data assessment and proteomics data availability

Validation of mRNA *CORO1A* levels was performed using a primary breast cancer dataset in the publicly available repository Human Cancer Metastasis Database (HCMDB; <http://hcmdb.i-sanger.com/index>). HCMDB consists of 124 previously published transcriptome datasets collected from Gene Expression Omnibus (GEO) and The Cancer Genome Atlas (TCGA). RNA expression status of *CORO1A* was evaluated in 204 GEO primary breast cancer samples available in the National Centre for Biotechnology Information (NCBI) under GEO accession number GSE12276. The Log₂ Medi-an-Centered ratio was used to evaluate the differential expression of *CORO1A* in primary breast cancer of patients who developed brain metastasis compared to patients who developed metastasis to other organs.

The mass spectrometry proteomics data have been deposited to the ProteomeXchange Consortium via the PRIDE¹⁰ partner repository. Dataset information is publicly available under GEO accession number GSE12276, EXP00013⁷. The data presented in this study are available in this article (and supplementary material).

Statistical analysis

Prism 5.0 (GraphPad Software) was used to perform statistical tests. A two-tailed Student's t-test was applied to find differences between the proteomes of the 3 cell lines prior to, and after incubation with activated T lymphocytes, or their CM. The identified proteins were sorted according to the significance levels following ANOVA testing. Data are presented as means \pm SD. In all statistical analyses, a p-value < 0.05 was considered statistically significant. Unless otherwise stated, in vitro experiments were repeated independently three times.

Results

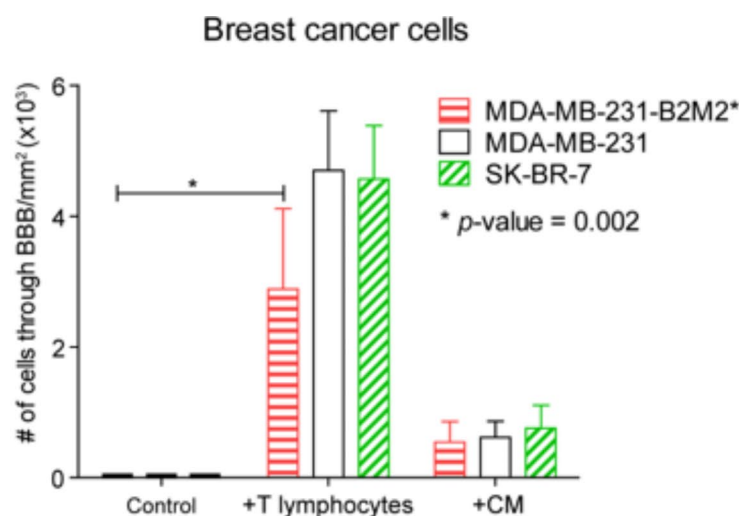
Activated T lymphocytes facilitate the BBB transmigration of all breast cancer cell lines

Co-culturing of the three breast cancer cell lines with activated T lymphocytes, or with activated T conditioned medium (CM), resulted in increased passage through the in vitro BBB (Fig. 1). The effects were less for cell line MDA-MB-231-B2M2 (brain affinity) as compared to MDA-MB-231 and SK-BR-7.

Differentially expressed proteins

To identify expressional changes in the three breast cancer cell lines upon either co-culture with activated T lymphocytes, or T lymphocyte CM, their proteomes were measured and compared. T cells were removed after incubation to exclude the presence of proteins expressed by T cells. T cell proteome were also analyzed separately and screened for specific T cell markers.

In total This led to the identification of an accumulated total of 4,542 proteins for the control cell lines, cocultures with T cell and CM and the used T cells separately from which 118 were specific for T cells and 169 specific for the CM incubation. The number of the various comparisons are displayed in Fig. 2. The numbers of identified proteins for each cell line are shown in Table 1.



* MDA-MB-231-B2M2 is the breast cancer cell line with metastasis predilection for brain.

Cell line	# cells ± SD			% increase		T-test (p-value)	
	Control	+ T lymphocytes	+ CM	+ T lymphocytes	+ CM	+ T lymphocytes	+ CM
MDA-MB-231-B2M2 *	2.3 ± 0.6	2884 ± 1230	545 ± 311	1236	233	0.002	0.008
MDA-MB-231	2.7 ± 2.9	4697 ± 910	618 ± 247	1761	231	<0.001	0.002
SK-BR-7	2.0 ± 1.0	4568 ± 820	758 ± 349	2283	379	<0.001	0.003

Fig. 1. BBB passage following co-culture with T cells or T cell medium. Co-culture of breast cancer cell lines with activated T lymphocytes stimulated passage of the cancer cells through the artificial BBB. The passage of MDA-MB-231-B2M2 cells was less than for MDA-MB-231 and SK-BR-7. The stimulating effect of T lymphocyte conditioned medium (CM) was grossly similar for all three cell lines and less than the effect of direct T cell contact. MDA-MB-231: ER-/PR-/Her2-/E-cadherin-/TP53^{mut} breast cancer cell line derived from invasive ductal carcinoma; MDA-MB-231-B2M2: derived from MDA-MB-231 with metastatic preference for brain; SK-BR-3: Her2+ breast cancer cell line from metastasizing tumor without specific organ preference. Control = matched cancer cells without pre-treatment; +T lymphocytes = cancer cells following five days of co-culture with activated T lymphocytes; + CM = cancer cells following five days incubation with cell-free media conditioned by activated T lymphocytes. Data representative of three independent experiments. For abbreviated cell lines see M&M.

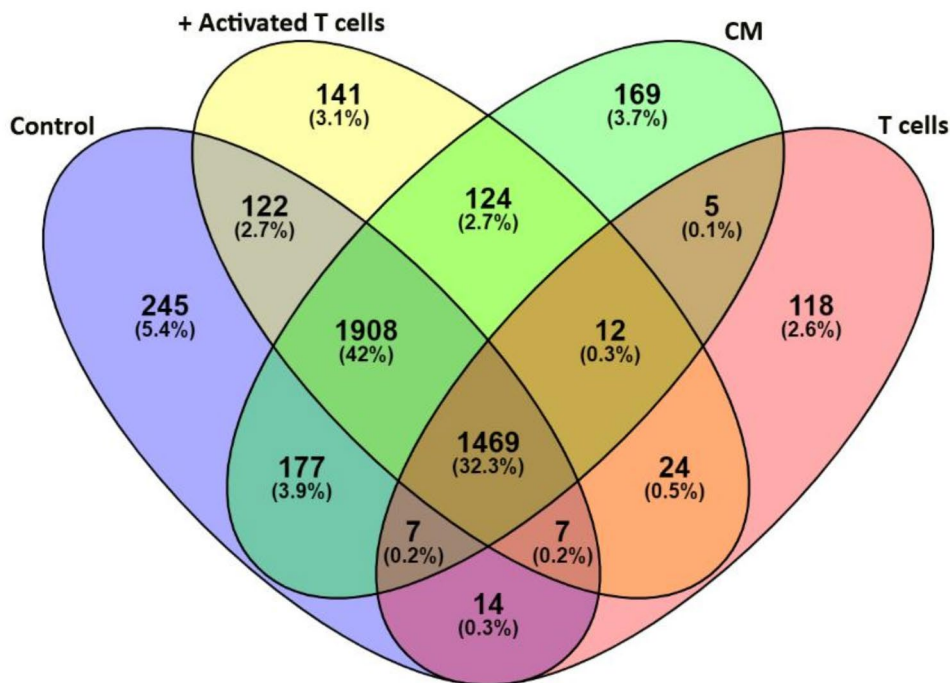


Fig. 2. Venn diagram of proteomics measurements. Total numbers of proteins measured in the cancer cell lines prior to, and incubation with activated T lymphocytes. 307 proteins were identified only in cancer cell lines after incubation with T lymphocytes.

Breast cancer cell line	Identified proteins of two measurements		
	Control	+ T lymphocytes	Overlap
MDA-MB-231-B2M2	3184	3287	2891
MDA-MB-231	3195	3070	2773
SK-BR-7	2991	2832	2575

Table 1. Number of proteins identified by LC-MS measurements.

MDA-MB-231: ER-/PR-/Her2-/E-cadherin-/TP53^{mut} breast cancer cell line derived from invasive ductal carcinoma; MDA-MB-231-B2M2: derived from MDA-MB-231 with metastatic preference for brain; SK-BR-3: Her2 + breast cancer cell line from metastasizing tumor without specific organ preference.

In total 153 proteins were differentially expressed (t-test, $p < 0.05$) in the breast cancer cell lines after T-lymphocyte contact (“control” vs. “+ T lymphocyte”). Detailed information is given in supplement Table S1. Subsequently, we focused on those proteins that were differentially expressed (ANOVA, $p < 0.05$) in the breast cancer cell lines after T-lymphocyte contact or T lymphocyte CM incubation and found that 35 of 153 proteins were differentially expressed ($P < 0.05$) (Table 2).

The comparison between each two groups (cells co-cultured with activated T cells vs. cells not co-cultured with activated T cells vs. cells with co-cultured conditioned media, and cells without activated T cells vs. cells co-cultured with conditioned media), was based on two sided t-test analysis, the p values of all proteins were considered differentially expressed if $p < 0.05$. Using Anova analysis, the proteins that were differentially expressed in the comparison between yes/no co-culturing were listed according to p-value (right column).

Coronin-1A overexpression in the breast cancer cells causes increased BBB transmigration following T lymphocyte contact

The coronin-1 A protein, known to relate to F-actin and cell motility, appeared to be significantly overexpressed in all three cancer cell lines after co-culture ($p = 0.014$) (Fig. 3a; Table 2).

Since coronin-1A plays a role in cell motility it was further studied at RNA level and in functional assays. In order to investigate the expression of the *CORO1A* mRNA levels we performed RT-PCR on the breast cancer

#	Protein name	Accession number	Molecular weight (kDa)	ANOVA test (p -value < 0.05)
1	Mitochondrial glutamate carrier 1	GHCI_HUMAN	34	0.00042
2	Peptidyl-prolyl cis-trans isomerase B	PPIB_HUMAN	24	0.0022
3	Interferon-induced transmembrane protein 1	IFM1_HUMAN	14	0.0035
4	Tubulin beta-6 chain	TBB6_HUMAN	50	0.0071
5	EF-hand domain-containing protein D2	EFHD2_HUMAN	27	0.0081
6	40 S ribosomal protein S10	RS10_HUMAN	19	0.013
7	HLA class I histocompatibility antigen, alpha chain E	HLAE_HUMAN	40	0.013
8	Coronin-1A	COR1A_HUMAN	51	0.014
9	Tubulin beta chain	TBB5_HUMAN	50	0.015
10	Tubulin beta-4 A chain	TBB4A_HUMAN	50	0.016
11	Chromodomain-helicase-DNA-binding protein 3	CHD3_HUMAN	227	0.016
12	Aconitate hydratase, mitochondrial	ACON_HUMAN	85	0.018
13	Tryptophan-tRNA ligase, cytoplasmic	SYWC_HUMAN	53	0.02
14	Rho GTPase-activating protein 35	RHG35_HUMAN	171	0.022
15	Proteasome subunit beta type-10	PSB10_HUMAN	29	0.022
16	Lysophospholipase-like protein 1	LYPL1_HUMAN	26	0.022
17	NADH dehydrogenase [ubiquinone] 1 subunit C2	NDUC2_HUMAN	14	0.022
18	COMM domain-containing protein 9	COMD9_HUMAN	22	0.024
19	TELO2-interacting protein 1 homolog	TTI1_HUMAN	122	0.026
20	Transmembrane protein 209	TM209_HUMAN	63	0.026
21	Probable ATP-dependent RNA helicase DDX47	DDX47_HUMAN	51	0.027
22	Pyrroline-5-carboxylate reductase 1, mitochondrial	P5CR1_HUMAN	33	0.03
23	Large proline-rich protein BAG6	BAG6_HUMAN	119	0.03
24	Condensin complex subunit 3	CND3_HUMAN	114	0.032
25	40 S ribosomal protein S12	RS12_HUMAN	15	0.033
26	Actin-related protein 2/3 complex subunit 3	ARPC3_HUMAN	21	0.034
27	General transcription factor II-I	GTF2I_HUMAN	112	0.035
28	Protein phosphatase 1 regulatory subunit 7	PP1R7_HUMAN	42	0.035
29	Vesicle-fusing ATPase	NSF_HUMAN	83	0.039
30	N-terminal kinase-like protein	NTKL_HUMAN	90	0.041
31	Putative HLA class I histocompatibility antigen, alpha chain H	HLAH_HUMAN	41	0.041
32	Protein HEXIM1	HEX11_HUMAN	41	0.043
33	Transcription elongation factor SPT5	SPT5H_HUMAN	121	0.045
34	Protein dpy-30 homolog	DPY30_HUMAN	11	0.045
35	Chromodomain-helicase-DNA-binding protein 5	CHD5_HUMAN	223	0.046

Table 2. Differentially expressed proteins in breast cancer cells following co-culture with activated T lymphocytes (Complete Table presented by Supplementary Table S1).

cell lines, which confirmed enhanced *CORO1A* expression (Fig. 3b). While the expression of *CORO1A* mRNA increased significantly ($p < 10^{-5}$) in the brain-trophic breast cancer cell line MDA-MB-231 when co-cultured with T lymphocytes in a setting that allowed direct cell-cell interactions, the *CORO1A* mRNA levels did not change when a 0.4 μm pore membrane physical barrier between both cell types was applied, or following incubation of the tumor cells with the T lymphocyte CM (Fig. 3a).

CORO1A knock-down in breast cancer cells impairs BBB transmigration ability

To validate the function of coronin-1 A in breast cancer cells, RNA knockdown (siRNA) experiments were conducted prior to BBB passage studies. Successful silencing of *CORO1A* in all three breast cancer cell lines was verified by measuring the mRNA levels (Fig. 4a). *CORO1A* knockdown significantly reduced (50–60%) the capacity of both brain-trophic breast cancer cell lines to pass the in vitro BBB ($p < 0.001$, Fig. 4b). The BBB passage capacity of the non-brain trophic breast carcinoma cell line SK-BR-7 cells also dropped, but this did not reach significance (Fig. 4b).

Immunofluorescence analysis (IF) of coronin-1A expression levels in the breast cancer cells revealed overexpression of coronin-1A after co-culture with T lymphocytes for all three breast cancer cell lines (Fig. 4c,d). The increase in expression in the brain-specific MDA-MB-231-B2M2 cells remained marginal (Fig. 4d). *CORO1A* siRNA reduced the coronin-1A IF intensity levels to half of the levels of matched control cells and this was observed for all three breast cancer cell lines (Fig. 4e,f).

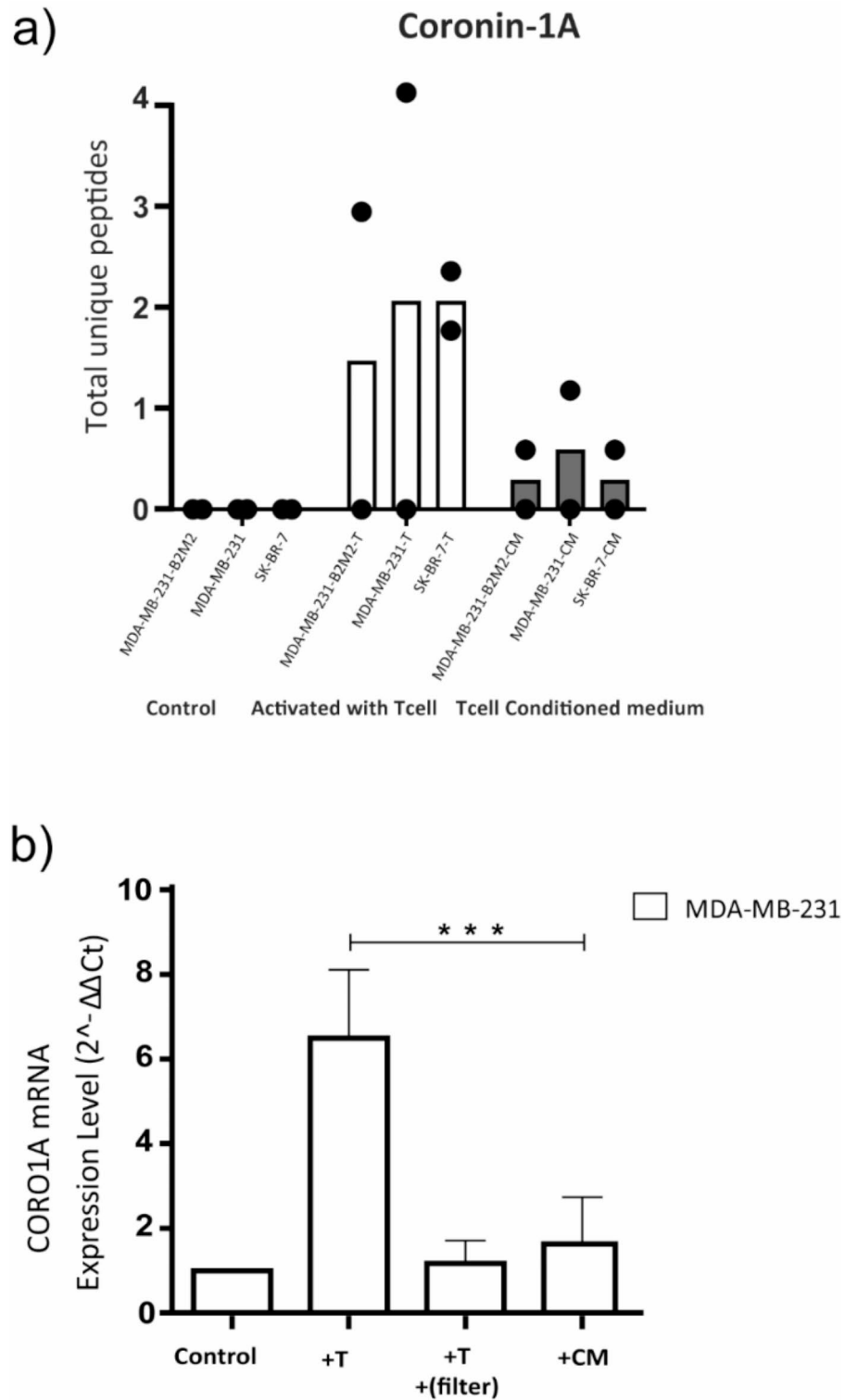


Fig. 3. Coronin-1 A is upregulated in breast cancer cells after contact with T lymphocytes. (a) Unique peptide counts for Coronin-1 A; (b) Elevated CORO1A mRNA expression levels in MDA-MB-231 cells following direct contact with activated T lymphocytes, or incubation with T cells separated from the tumor cells with a 0.4 micron filter, or with CM of activated T lymphocytes. *Control* = matched cancer cells without pre-treatment; *+ T* = cancer cells after 5 days of co-culture with activated T lymphocytes, *+ CM* = cancer cells after 5 days incubation with cell-free media conditioned by activated T lymphocytes.

Primary breast cancers from patients with brain metastasis overexpress coronin-1A

Analysis of coronin-1A protein in primary breast cancer samples clearly showed significantly higher coronin-1A expression levels in primary breast cancer samples of patients who developed brain metastasis than those observed in breast cancer tissue samples of patients who had metastases in organs other than brain ($p=0.0035$; Fig. 5a-c). *CORO1A* mRNA analysis revealed a trend towards expression levels in primary breast cancer samples of patients who developed brain metastasis, but was not significant (Fig. 5b).

In an online mRNA expression database of 204 primary breast cancers we noticed that *CORO1A* mRNA levels were significantly higher in tumors that specifically and only metastasized to brain ($p=0.023$, Fig. 5d).

Discussion

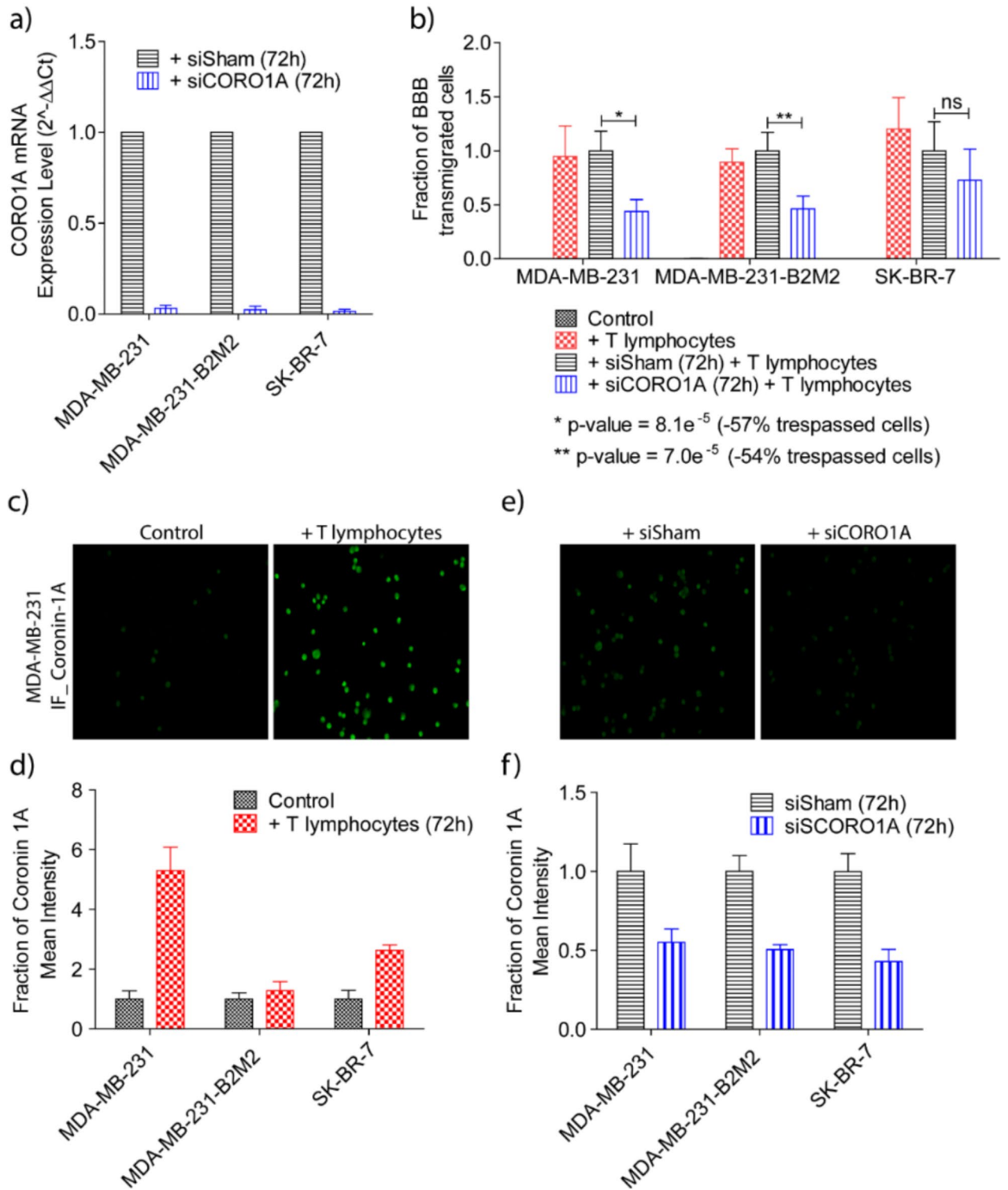
In this study we identified 35 proteins that appeared to be upregulated in breast cancer cells upon contact with activated T lymphocytes, resulting in their accelerated passage through the BBB model. Notoriously, the expression of the cell motility-related protein coronin-1A rose from virtually zero to high levels upon co-culturing with activated T lymphocytes. Levels of coronin-1A were not elevated following indirect co-culture, i.e. co-culture while not allowing physical contact between the cancer cells and the T lymphocytes. In addition, coronin-1A levels in the cancer cells also remained low following incubation with activated T-lymphocyte conditional medium. This data suggests that direct cellular interaction between cancer cells and T lymphocytes is a requirement for the upregulation in the breast cancer cells. How breast cancer cells exploit the T lymphocytes and their secreted factors to more efficiently transmigrate through the BBB remains unclear. Various molecular cascades related to cell motility have been associated with passage through the BBB^{13–15}. The current data suggest that the immune system, T lymphocyte effects in particular, also play a role in this, possibly by enhancing cellular motility of breast cancer cells.

Coronins are actin-branching regulators binding to F-actin and the ARP2/3 complex required for dimerization and filament bundling^{16,17}. Type I coronins (1A, 1B and 1C) localize to actin-rich cellular structures serving a wide variety of cellular processes, among which cell motility¹⁰. By interactions with F-actin they alter lamellipodia by which they steer cellular migration^{10,11}. We only found coronin-1A to be upregulated following T lymphocyte contact while the expression of its family members coronin-1B, coronin 1C and coronin 7 remained unaffected. In our in vitro BBB model we found that silencing of *CORO1A* significantly reduced BBB transmigration of the breast cancer cells. The finding that silencing of *CORO1A* reduces the BBB transmigration of the brain trophic breast cancer cell lines MDA-MB-231 by more than 50% while silencing *CORO1A* in the non-brain trophic SK-BR-7 cells did not significantly impair transmigration, points to cell-lineage differences in molecules and pathways exploited for BBB passage. Moreover, silencing of coronin-1A did not completely block the transmigration of cells through the BBB in any of the three breast cancer cell lines explored, suggesting that other molecular mechanisms are also operative in the migration process.

We have demonstrated that direct cellular contact between activated T lymphocytes and breast cancer cells is crucial for enhanced BBB transmigration, which corresponds to the increased development of brain metastasis observed in breast carcinoma⁵. The role of the immune system in tumorigenesis is complex and to some extent contradictory. Initial progression of cancer is associated with immune suppression, while at later stages the immune system seems hijacked and abused by the tumor cells. For the initial stages immune checkpoint inhibitors (ICIs) have been developed to reactivate immune pathways that harbor immunosuppressive functions and promote the activation and proliferation of effector T lymphocytes for efficient cancer cell elimination¹⁸. Various reports have shown clinical benefits from ICI treatment for patients with brain metastatic malignancies^{19–22}, although the effects on prognosis of patients treated with ICIs are not equivocal²³. The interference of ICIs with T lymphocyte biology and the effects on the development of brain metastasis in cancer patients remain unclear, and should be addressed in in vitro BBB functional assays as well as in vivo brain metastatic mouse models.

Conclusions

Activated T lymphocytes increase the ability of breast cancer cell lines to cross an artificial BBB, which involves the induction of coronin-1A expression in the breast cancer cells. The effects of T lymphocytes on BBB passage are strongest on the cell lines lacking intrinsic brain affinity. The results illustrate the influence of immune cells on the breast cancer proteome and contribute to new avenues of therapeutic interventions preventing the rise of breast cancer brain metastasis.



◀ **Fig. 4.** *CORO1A* siRNA impairs the BBB passage in all three breast cancer cell lines. (a) *CORO1A* mRNA levels in all three breast cancer cell lines before and after *CORO1A* siRNA for 72 h. mRNA expression is reduced to almost undetectable in all three cell lines. Data representative of two independent experiments. (b) Fraction of breast cancer cells passing the BBB before and following siRNA *CORO1A* and subsequent co-culture with activated T lymphocytes. The fraction of cancer cells not silenced for *CORO1A* (siSham) are taken as fraction = 1. The fractions of crossing cells are significantly reduced for MDA-MB-231 and MDA-MB-231-B2M2. The fraction of SK-BR-7 cells decreased, though not significantly. Data representative of two independent experiments. (c) Coronin-1A immunofluorescence (IF) of MDA-MB-231 without (left) and after (right) co-culture with activated T lymphocytes. The cancer cells express coronin-1A upon T cell contact. (d) Coronin 1A-IF FOC intensity-levels in the breast cancer cell lines before and after 72 h of co-culture with activated T lymphocytes. For cell line MDA-MB-231 and SK-BR-7 upregulation is robust, but remains marginal in MDA-MB-231-B2M2 (data representative of three independent experiments). (e) Example of coronin-1A-IF of MDA-MB-231 siSham cells (left) and of MDA-MB-231 si*CORO1A* following co-culture with activated T lymphocytes (right). (f) Coronin 1A protein fraction levels before and after 72 h incubation with non-targeting siSham or siRNA *CORO1A* were equally reduced in all three cell lines. Data representative of three independent experiments.

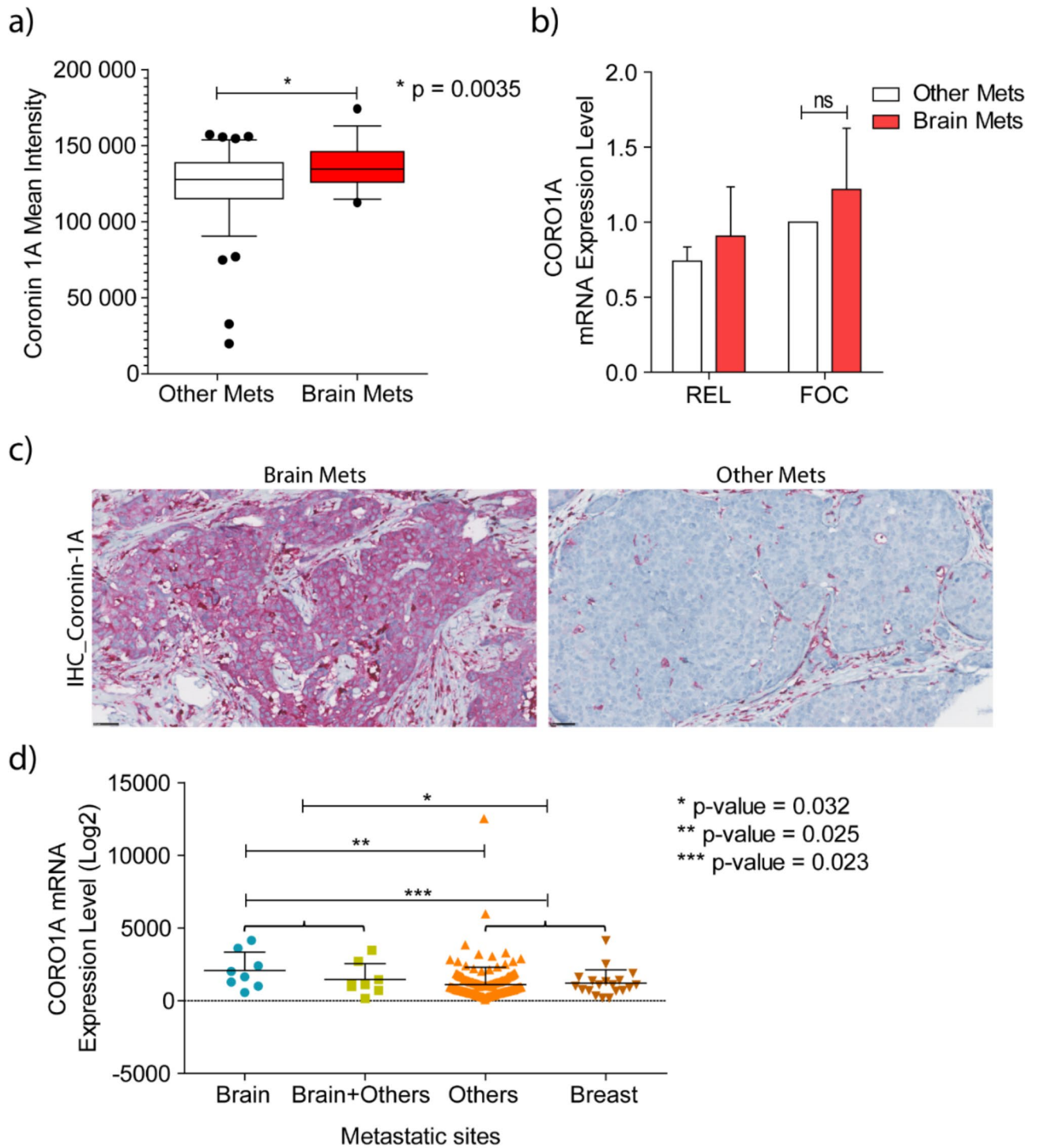


Fig. 5. Coronin 1A is highly expressed in primary breast cancers from patients who developed brain metastases. **(a)** Coronin 1A immunohistochemistry mean-intensity levels are significantly higher in the group of breast cancers from patients who developed brain metastasis ($n = 10$, Brain Mets) when compared with breast cancers from patients with metastases to organs other than brain ($n = 22$, Other Mets), $p = 0.0035$. The lowest and highest boundaries of the box represent the 25 and 75 percentiles, respectively. The solid line across the box indicates the median value. Error bars indicate the 5–95 percentile. **(b)** *CORO1A* mRNA relative (REL) and fold of change (FOC) expression levels in the two groups described in a), $p > 0.05$. **(c)** Example of coronin-1A IHC of primary breast cancers from patients who developed brain metastasis (left) or metastasis to other organs than brain (right). **(d)** *CORO1A* mRNA expression levels of 204 primary breast cancers associated with different sites of metastasis: brain ($n = 8$); brain and other organs ($n = 8$); other metastatic organs ($n = 169$) and metastasis to the contralateral breast ($n = 19$). Dataset information is publicly available under GEO accession number GSE12276, EXP00013 [37].

Data availability

Data is provided within the manuscript or supplementary information files. Validation of mRNA CORO1A levels was performed using a primary breast cancer dataset in the publicly available repository Human Cancer Metastasis Database (HCMDB; <http://hcmdb.i-sanger.com/index>). HCMDB consists of 124 previously published transcriptome datasets collected from Gene Expression Omnibus (GEO) and The Cancer Genome Atlas (TCGA). RNA expression status of CORO1A was evaluated in 204 GEO primary breast cancer samples available in the National Centre for Biotechnology Information (NCBI) under GEO accession number GSE12276. The Log2 Median-Centered ratio was used to evaluate the differential expression of CORO1A in primary breast cancer of patients who developed brain metastasis compared to patients who developed metastasis to other organs. The mass spectrometry proteomics data have been deposited to the ProteomeXchange Consortium via the PRIDE [20] partner repository. Dataset information is publicly available under GEO accession number GSE12276, EXP00013 [7]. The data presented in this study are available in this article (and supplementary material).

Received: 27 June 2024; Accepted: 13 December 2024

Published online: 28 December 2024

References

- Schouten, L. J. et al. Incidence of brain metastases in a cohort of patients with carcinoma of the breast, colon, kidney, and lung and melanoma. *Cancer* **94** (10), 2698–2705 (2002).
- Hatiboglu, M. A., Akdur, K. & Sawaya, R. Neurosurgical management of patients with brain metastasis. *Neurosurg. Rev.* **43** (2), 483–495 (2020).
- Lassman, A. B. & DeAngelis, L. M. Brain metastases. *Neurol Clin.* **21**(1), 1–23, vii (2003).
- Barnholtz-Sloan, J. S. et al. Incidence proportions of brain metastases in patients diagnosed (1973 to 2001) in the Metropolitan Detroit Cancer Surveillance System. *J. Clin. Oncol.* **22** (14), 2865–2872 (2004).
- Mustafa, D. A. M. et al. T lymphocytes facilitate brain metastasis of breast cancer by inducing Guanylate-Binding Protein 1 expression. *Acta Neuropathol.* **135** (4), 581–599 (2018).
- Cailleau, R., Olive, M. & Cruciger, Q. V. Long-term human breast carcinoma cell lines of metastatic origin: preliminary characterization. *In Vitro* **14** (11), 911–915 (1978).
- Bos, P. D. et al. Genes that mediate breast cancer metastasis to the brain. *Nature* **459** (7249), 1005–1009 (2009).
- Alper, O. et al. The presence of c-erbB-2 gene product-related protein in culture medium conditioned by breast cancer cell line SK-BR-3. *Cell. Growth Differ.* **1** (12), 591–599 (1990).
- Eugenin, E. A. & Berman, J. W. Chemokine-dependent mechanisms of leukocyte trafficking across a model of the blood-brain barrier. *Methods* **29** (4), 351–361 (2003).
- Perez-Riverol, Y. et al. The PRIDE database and related tools and resources in 2019: improving support for quantification data. *Nucleic Acids Res.* **47** (D1), D442–D450 (2019).
- Schneider, C. A., Rasband, W. S. & Eliceiri, K. W. NIH Image to ImageJ: 25 years of image analysis. *Nat. Methods.* **9** (7), 671–675 (2012).
- Pedrosa, R. M. S. M. et al. Differential expression of BOC, SPOCK2, and GJD3 is associated with brain metastasis of ER-negative breast cancers. *Cancers*, **13**(12). (2021).
- Pedrosa, R. et al. Potential molecular signatures predictive of lung cancer brain metastasis. *Front. Oncol.* **8**, 159 (2018).
- Lin, C. Y. et al. ADAM9 promotes lung cancer metastases to brain by a plasminogen activator-based pathway. *Cancer Res.* **74** (18), 5229–5243 (2014).
- Pedrosa, R. et al. Breast cancer brain metastasis: molecular mechanisms and directions for treatment. *Neuro Oncol.* **20** (11), 1439–1449 (2018).
- Goode, B. L. et al. Coronin promotes the rapid assembly and cross-linking of actin filaments and may link the actin and microtubule cytoskeletons in yeast. *J. Cell. Biol.* **144** (1), 83–98 (1999).
- Humphries, C. L. et al. Direct regulation of Arp2/3 complex activity and function by the actin binding protein coronin. *J. Cell. Biol.* **159** (6), 993–1004 (2002).
- Darvin, P. et al. Immune checkpoint inhibitors: recent progress and potential biomarkers. *Exp. Mol. Med.* **50** (12), 1–11 (2018).
- Du, W. et al. A retrospective study of brain metastases from solid malignancies: the effect of immune checkpoint inhibitors. *Front. Oncol.* **11**, 667847 (2021).
- Nunno, V. D. et al. Clinical efficacy of immune checkpoint inhibitors in patients with brain metastases. *Immunotherapy* **13** (5), 419–432 (2021).
- Goldberg, S. B. et al. Pembrolizumab for patients with melanoma or non-small-cell lung cancer and untreated brain metastases: early analysis of a non-randomised, open-label, phase 2 trial. *Lancet Oncol.* **17** (7), 976–983 (2016).
- Kamath, S. D. & Kumthekar, P. U. Immune checkpoint inhibitors for the treatment of central nervous system (CNS) metastatic disease. *Front. Oncol.* **8**, 414 (2018).
- Hu, X. et al. Immune checkpoint inhibitors and survival outcomes in brain metastasis: a time series-based meta-analysis. *Front. Oncol.* **10**, 564382 (2020).

Acknowledgements

The authors thank Dr. C. Berrevoets and prof. R. Debets for providing T cells for the co-culture experiments. Dr. I. Hadries is thanked for his assistance with the PCR runs. Mrs. M. Brakel, department of Medical Oncology, Erasmus MC, for helping to provide activated T lymphocytes; P.A.R.T.S. (www.parts-erasmusmc.nl/) for performing the IHC and IF, and MSc. W. de Koning, Pathology department, Erasmus MC, for his help with extracting publicly available databases.

Author contributions

R.M.S.M.P., J.M.K. and D.A.M.M. conceptualized and contributed to the methodology of the manuscript; R.M.S.M.P. performed the formal analysis and validated the results; L.Z., Z.B. and T.M.L. contributed actively to the processing and interpretation of the proteomics analysis; R.M.S.M.P. wrote and L.Z., T.M.L., W.A.D., J.M.K. and D.A.M.M. edited the manuscript; All authors read and approved the final manuscript.

Funding

This work was partially funded by the Dutch Cancer Society (KWF), grant number EMCR 2009–4553; by the Department of Pathology, Erasmus MC; by Stichting Support Casper.

Declarations

Consent for publication

All authors have seen and approved the text for publication.

Competing interests

The authors declare no competing interests.

Ethics approval and consent

Institutional Review Board Statement: This study was approved by the Medical Ethics Committee of the Erasmus Medical Center, Rotterdam, The Netherlands (MEC 02-953) and performed in adherence to the Code of Conduct of the Federation of Medical Scientific Societies in the Netherlands (<http://www.fmwv.nl/>).
Informed Consent Statement: Informed consent was obtained from all subjects involved in the study.

Additional information

Supplementary Information The online version contains supplementary material available at <https://doi.org/10.1038/s41598-024-83301-x>.

Correspondence and requests for materials should be addressed to J.M.K.

Reprints and permissions information is available at www.nature.com/reprints.

Publisher's note Springer Nature remains neutral with regard to jurisdictional claims in published maps and institutional affiliations.

Open Access This article is licensed under a Creative Commons Attribution-NonCommercial-NoDerivatives 4.0 International License, which permits any non-commercial use, sharing, distribution and reproduction in any medium or format, as long as you give appropriate credit to the original author(s) and the source, provide a link to the Creative Commons licence, and indicate if you modified the licensed material. You do not have permission under this licence to share adapted material derived from this article or parts of it. The images or other third party material in this article are included in the article's Creative Commons licence, unless indicated otherwise in a credit line to the material. If material is not included in the article's Creative Commons licence and your intended use is not permitted by statutory regulation or exceeds the permitted use, you will need to obtain permission directly from the copyright holder. To view a copy of this licence, visit <http://creativecommons.org/licenses/by-nc-nd/4.0/>.

© The Author(s) 2024